Cell Death and Differentiation (2010) 17, 1529–1539

www.nature.com/cdd

Cathepsin B facilitates autophagy-mediated apoptosis in SPARC overexpressed primitive neuroectodermal tumor cells

P Bhoopathi[1], C Chetty[1], M Gujrati[2], DH Dinh[3], JS Rao[1,3] and S Lakka*[,1]

Medulloblastoma and neuroblastoma belong to a group of neoplasms designated as primitive neuroectodermal tumors (PNETs). Secreted protein, acidic and rich in cysteine (SPARC) is a matrix-associated glycoprotein that influences a variety of cellular activities *in vitro* and *in vivo*. In this study, we provide evidence that expression of SPARC cDNA induces autophagy in PNET cells followed by apoptotic cell death. SPARC-induced autophagy was morphologically characterized by (i) the formation of membrane-bound autophagic vacuoles (AVOs), (ii) increase in the levels of microtubule-associated protein light chain 3 (LC3) and (iii) induction of the lysososmal enzyme cathepsin B. Cathepsin B, in turn induced mitochondrial release of cytochrome c and activated caspase-3, events that signify the onset of apoptotic cell death. In agreement with these observations, inhibition of autophagy by 3-MA reduced AVO formation and LC3 and inhibited apoptosis, suggesting that autophagy has a role in SPARC-mediated apoptosis. Blocking cathepsin B expression with a specific inhibitor of cathepsin B suppressed apoptosis but did not affect autophagy, which suggests that cathepsin B is a molecular link between autophagy and apoptosis. In summary, these findings show that SPARC expression induces autophagy, which results in the elevation of cathepsin B and subsequent mitochondria-mediated apoptosis.
Cell Death and Differentiation (2010) **17,** 1529–1539; doi:10.1038/cdd.2010.28; published online 26 March 2010

Autophagy is an intracellular, lysosome-mediated catabolic mechanism that is responsible for the bulk degradation and recycling of damaged or dysfunctional cytoplasmic components and intracellular organelles.[1] It is an evolutionarily ancient cellular response to intra- and extracellular noxious stimuli, which may precede or coexist with apoptosis, and it may be induced by apoptotic stimuli.[2] Autophagy serves to maintain cellular metabolism through recycling of cellular components when the availability of external nutrient sources is limited. In contrast, autophagy develops as a primary response to stress stimuli and then triggers either apoptosis or necrotic cell death.[3] The functional relationship between apoptosis and autophagy is complex in the sense that the type of the initiating stimulus might determine which process will dominate. For example, during nutrient deprivation, the default pathway would be autophagy, which creates a metabolic state with high (or increased) ATP and is anti-apoptotic.[4] Successful removal of damaged organelles, followed by repair and adaptation, would allow for survival, whereas failure to restore homeostasis would result in delayed apoptosis. By contrast, the default pathway that is triggered by other signals such as DNA damage or death-receptor activation would be immediate apoptosis, which occurs in a rapid, self-amplifying process, precluding simultaneous autophagic responses. As in normal cells, autophagy is activated in tumor cells by stress, including starvation, hypoxia and factor deprivation,[5] which enables long-term survival, particularly when apoptosis is defective.[6,7] However, tumor cells were shown to have less potential to induce autophagy or to suppress consumption in response to stress, which can lead to metabolic catastrophe in which energetic demand exceeds production.[8] This metabolic fragility of tumor cells has suggested therapeutic starvation as an approach to cancer therapy to exploit an inherent difference between normal and tumor cells.[9] Several studies indicate that although autophagy supports tumor cell survival, many tumors may paradoxically have autophagy suppressed.[10] Therefore, establishing how the functional status of autophagy influences tumorigenesis and treatment response has clinical implications.

Primitive neuroectodermal tumors (PNETs) of the central nervous system, such as neuroblastoma and medulloblastoma, still present a therapeutic challenge and require novel treatment approaches. Differential expression of secreted protein acidic rich in cysteine (SPARC) has been observed in various human cancers, and it is unclear why it has variable effects on tumor growth in different tissues. SPARC appears to function as a tumor suppressor in ovarian

[1]Program of Cancer Biology, Department of Cancer Biology and Pharmacology, University of Illinois College of Medicine at Peoria, One Illini Drive, Peoria, IL 61605, USA; [2]Department of Pathology, University of Illinois College of Medicine at Peoria, One Illini Drive, Peoria, IL 61605, USA and [3]Department of Neurosurgery, University of Illinois College of Medicine at Peoria, One Illini Drive, Peoria, IL 61605, USA
*Corresponding author: S Lakka, Department of Cancer Biology and Pharmacology, University of Illinois College of Medicine at Peoria, One Illini Drive, Peoria, IL 61605, USA. Tel: +309 671 3445; Fax: +309 671 3442; E-mail: slakka@uic.edu
Keywords: SPARC; apoptosis; autophagy; cathepsin B; PNET; Bid
Abbreviations: PNETs, primitive neuroectodermal tumors; SPARC, secreted protein, acidic and rich in cysteine; AVOs, membrane-bound autophagic vacuoles; LC3, microtubule-associated protein light chain 3
Received 28.8.09; revised 26.1.10; accepted 29.1.10; Edited by D Rubinsztein; published online 26.3.10

cancer,[11] pancreatic cancer[12] and acute myeloid leukemia.[13] Moreover, in tumor xenograft models, a greater growth of pancreatic cancer cells was observed in SPARC−/− mice in comparison with wild type SPARC +/+.[12] Previous studies have shown that SPARC retards the growth of tumors through its ability to enhance apoptosis. This has been shown in studies in which exogenous exposure to SPARC resulted in enhanced apoptosis in ovarian cancer cells,[11] whereas its absence endogenously diminished this event.[12] The aim of this study was to determine the functional significance of SPARC expression in PNET cells. In addition, we examined the possible mechanisms by which SPARC expression might elicit therapeutic responses in PNET cells. To address these aims, we used an adenovirus construct expressing full-length SPARC cDNA to induce SPARC expression in human medulloblastoma and neuroblastoma cell lines and studied its effect on cell death. We show that SPARC expression-induced autophagy followed by mitochondria-dependent apoptotic cell death.

Results

Ad-DsRed-SP infection-induced SPARC mRNA transcription in PNET cells. We constructed an E1/E3-defective recombinant adenovirus encoding the *SPARC* gene under the control of the immediate early promoter from cytomegalovirus (Ad-DsRed-SP). The replication-deficient vector, which encodes the *RFP* gene under the CMV controls (Ad-DsRed), served as the empty vector adenovirus control. To confirm expression of the SPARC protein from the engineered adenovirus, we infected PNET cells (medulloblastoma and neuroblastoma cells) with virus-containing culture supernatants. Western blotting and RT-PCR analysis of SPARC protein and mRNA, respectively, in medulloblastoma and neuroblastoma cells revealed that adenoviral-mediated delivery of the SPARC cDNA to PNET cells markedly enhanced the expression of SPARC protein and mRNA in a dose-dependent manner as compared with mock and Ad-DsRed-infected controls. Figure 1a shows that at 100 MOI, SPARC protein and mRNA levels increased up to approximately threefold ($P<0.01$ *versus* Ad-DsRed control) and approximately three- to fourfold ($P<0.01$ *versus* Ad-DsRed control), respectively.

SPARC overexpression increased sub-G1 peaks and TUNEL-positive cells in tumor cells. Quantitative evaluation of apoptosis was performed by FACS analysis of PNET cells infected with various doses of Ad-DsRed-SP and compared with mock and Ad-DsRed controls. DNA frequency distribution histograms in which the sub-G1 region corresponded to apoptotic cells indicated that Ad-DsRed-SP infection increased the number of apoptotic cells by 49.15 ± 2.25%, 56.7 ± 4% and 53.4 ± 2.24% with 100 MOI in Daoy, D283 and SH-SY5Y cells, respectively, as compared with 5.0 ± 2% in Ad-DsRed-infected controls (Figure 2a, Supplementary Figure 1). In addition, SPARC significantly increased TUNEL-positive apoptotic cells in medulloblastoma and neuroblastoma cells in a concentration-dependent manner (Figure 2b, Supplementary Figure 2) In addition, we also show that SPARC expression disrupts mitochondrial

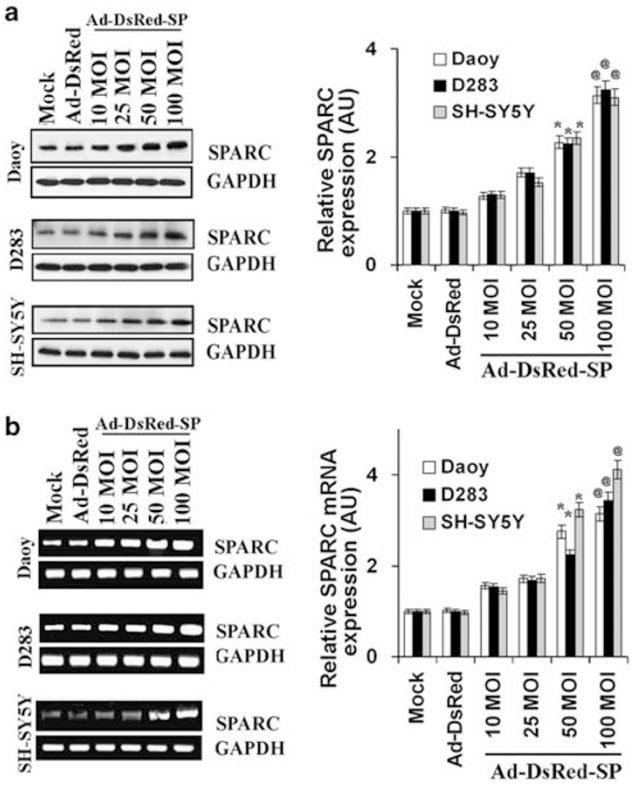

Figure 1 Overexpression of SPARC in PNET cells. The human full-length SPARC cDNA was cloned into the Adeno-X ViraTrak DsRed Expression System, termed as Ad-DsRed-SP, and Ad-DsRed is the viral vector without the SPARC gene. DAOY, D283 and SH-SY5Y cells (PNET cells) were infected with mock (PBS control), 100 MOI of Ad-DsRed and the indicated MOI (10, 25, 50 and 100 MOI) of Ad-DsRed-SP for 48 h. (**a**) SPARC levels were determined by western blot analysis using SPARC-specific antibody. GAPDH served as loading control. (**b**) cDNA was produced from total RNA extracted from the mock and infected cells. RT-PCR was performed for SPARC. Results are representative of three independent experiments. GAPDH served as a control for RNA quality (columns, mean of three experiments; bars, S.D.). *$P<0.05$, difference between Ad-DsRed and Ad-DsRed-SP 50 MOI treatment; @$P<0.01$, difference between Ad-DsRed and Ad-DsRed-SP 100 MOI

membrane potential in PNET tumor cells (Supplementary Figure 3), an early event in apoptosis.[14] In this study, SPARC expression-induced cleavage of caspases-8, -3 and poly-ADP-ribose polymerase (PARP) (Figure 2c) and released cytochrome c into cytosol (Figure 2d), in medulloblastoma and neuroblastoma cells in a dose-dependent manner. Further, SPARC overexpression in PNET cells increased Bid cleavage (t-Bid; Figure 2d) and, caspase-3 and -8 activity in a dose-dependent manner when compared with mock or Ad-DsRed controls (Figure 2e). These results indicate that SPARC expression-induced apoptosis in PNET cells.

SPARC overexpression induces autophagy vacuoles (AVOs) in neuroblastoma and medulloblastoma cells. We next sought to determine the sequential biological events connecting SPARC expression and apoptosis. Inspection of SPARC overexpressed cells under light microscopy revealed the presence of microscopic vacuoles, which formed as early as 12 h of after infection with Ad-DsRed-SP. The formation of

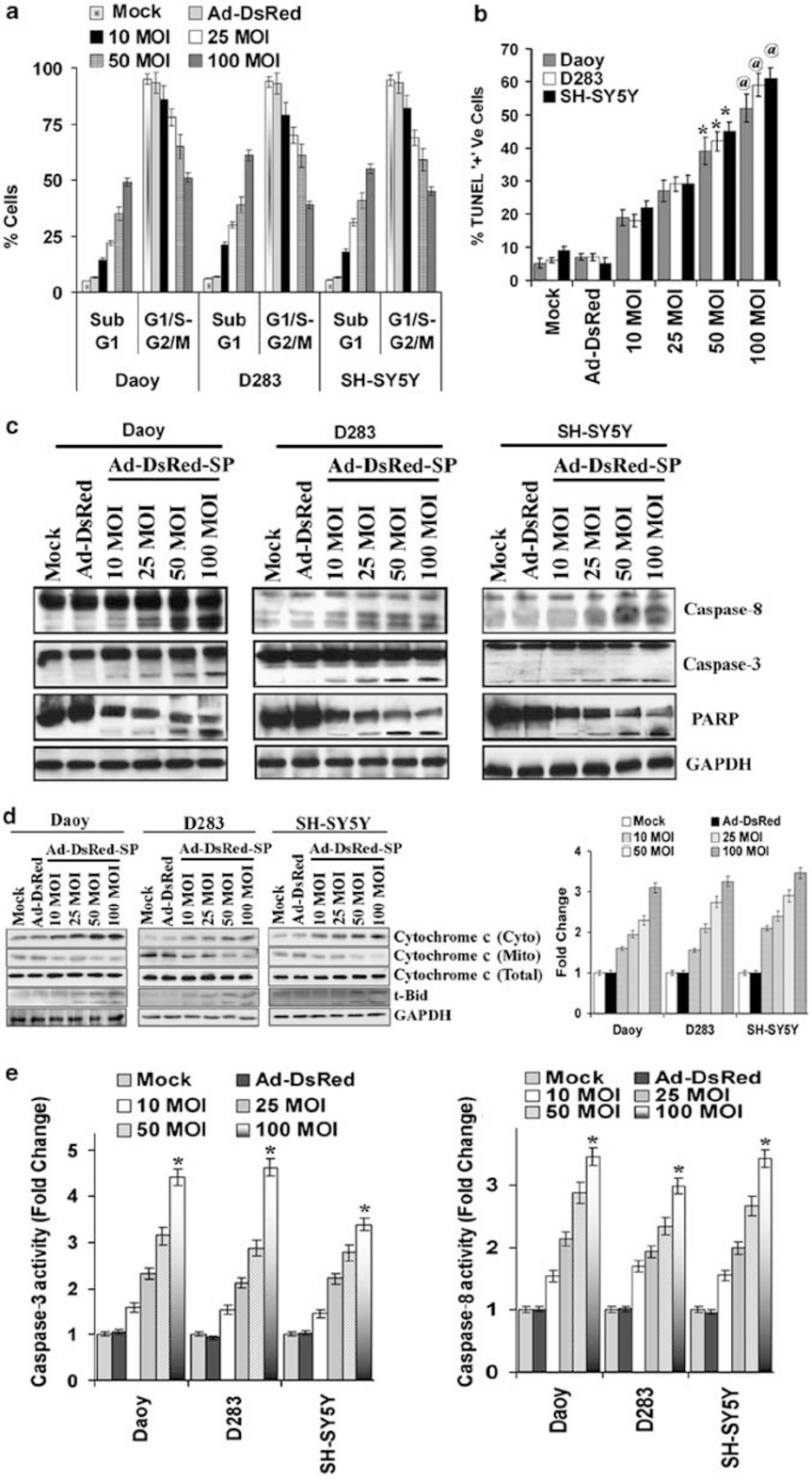

Figure 2 SPARC induces apoptosis in PNET cells. PNET cells were infected with mock, 100 MOI of Ad-DsRed and the indicated MOI of Ad-DsRed-SP for 48 h. (**a**) The degree of apoptosis was determined by flow cytometry using propidium iodide staining of hypodiploid DNA content. (**b**) Apoptosis was detected by the dUTP nick end labeling assay (TUNEL). (**c**) Cell lysates were assessed for caspases-8 and -3 and PARP cleavage levels by western blotting. (**d**) Cell lysates, mitochondrial and cytosolic fractions were assessed for cytochrome c and t-Bid levels by western blotting. Results are representative of three independent experiments. GAPDH served as a loading control (columns, mean of three experiments; bars, S.D.). *$P<0.05$, difference between Ad-DsRed and Ad-DsRed-SP 50 MOI treatment; $^{@}P<0.01$, difference between Ad-DsRed and Ad-DsRed-SP 100MOI

vacuoles was apparent when compared with the mock and Ad-DsRed control. SPARC expression clearly induced the accumulation of AVOs with their characteristic double membranes, as visible by transmission electron microscopy (Supplementary Figure 4). Autophagy is characterized by AVO formation, and measured by vital staining of acridine orange. Acridine orange moves freely to cross biological membranes and accumulates in acidic compartment, in which it is observed as fluorescence bright red.[15] Vital staining of PNET cells with acridine orange showed the accumulation of AVO in the cytoplasm of cells infected with Ad-DsRed-SP compared with controls (Supplementary Figure 5). Evaluation of autophagy was further performed through analysis of microtubule-associated protein I light chain 3 (LC3) expression, which is a reliable marker of autophagosomes.[16] Immunoblot analyses of proteins from Ad-DsRed-SP-infected cells revealed a dose-dependent increase in the expression of LC3-II (15 kDa), a surface protein marker of autophagosomes, which is ultimately degraded by acidic hydrolases after the formation of autolysosomes in PNET cells (Figure 3a).[17] To further confirm that SPARC overexpression induces autophagy PNET cells were treated with bafilomycin A1, a vacuolar type H^+-ATPase inhibitor, with or without Ad-DsRed-SP treatment and the accumulation of LC3-II protein was determined. Western blot showed that bafilomycin A1 increased the protein levels of LC3-II in a dose-dependent manner (Figure 3b).

The process of autophagosome formation is regulated by several autophagy genes (Atgs), Atg-5 or Atg-6/Beclin-1.[18] Therefore, the interconnection between SPARC-induced autophagy and apoptosis was further analyzed using Atg-5-specific siRNA and 3-methyl adenine (3-MA), a pharmacologic inhibitor of autophagy, a nucleotide derivative that blocks class III PI3K activity.[19] Transfection with Atg-5 siRNA inhibited autophagy and significantly decreased caspase-8, -3 ($P<0.05$) and PARP cleavage ($P<0.01$; Figure 3c) and the activity levels of caspase-8, -3 (Supplementary Figures 6 and 7). Further, Atg-5 siRNA tranfection decreased TUNEL-positive cells (Supplementary Figure 8) in Ad-DsRed-SP-infected cells (Figure 3c). Similarly, treatment with 3-MA also decreased cleavage of caspase-3 ($P<0.05$) and PARP ($P<0.05$) and inhibited the activity levels of caspase-8, -3, (Supplementary Figure 6 and 7) as well as TUNEL-positive cells (Supplementary Figures 8 and 9) in Ad-DsRed-SP-infected cells. Collectively, these results suggested that autophagy precedes apoptosis in SPARC-overexpressed PNET cells.

Cathepsin B mediates SPARC-induced apoptosis in PNET cells. There is growing recognition that alternative proteolytic enzymes, such as the lysosomal cathepsin proteases, can initiate or propagate pro-apoptotic signals.[20,21] We therefore determined the expression of cathepsins in Ad-DsRed-SP-infected PNET cells. Figure 4a shows that SPARC expression induced a dose-dependent increase in cathepsin B but not in cathepsins D or L as determined by western blotting. In addition, SPARC expression induced a three- to four-fold increase in cathepsin B activity levels in all the three cell lines compared with mock and Ad-DsRed controls (Figure 4b). To further validate the role of autophagy in cathepsin B induction, we treated Ad-DsRed-SP-infected cells with the autophagy inhibitor Atg-5 siRNA or 3-MA. Atg-5 siRNA treatments and 3-MA clearly reversed SPARC-induced cathepsin B protein (Figures 3c and 4c) expression and activity (Supplementary Figure 10). The role of cathepsin B in SPARC-induced apoptosis was determined by treating Ad-DsRed-SP-infected cells with the cathepsin B-specific inhibitor CA-074 Me. Figure 4d shows that cathepsin B inhibition did not alter LC3-II expression, indicating that cathepsin B is not involved in SPARC-induced autophagy. However, cathepsin B inhibition significantly reduced the SPARC-induced apoptosis as shown by a decrease in the levels of cleaved caspase-3 ($P<0.05$) and cleaved PARP ($P<0.05$) compared with Ad-DsRed-SP-infected cells treated with DMSO and reversed SPARC-induced apoptotic index (Supplementary Figure 11). These findings confirm the pivotal role of cathepsin B in cell death induced by SPARC in PNET cells.

BID as putative cathepsin B target in SPARC-induced apoptosis. In some cell types, cathepsin B-initiated apoptosis occurs by a process associated with mitochondrial release of cytochrome c.[22] We therefore determined whether SPARC-induced apoptosis involves this pathway in PNET cells infected with Ad-DsRed-SP and assessed whether cathepsin B was upstream of mitochondrial involvement. The levels of cytosolic cytochrome c were evaluated by immunoblotting. As shown in Figure 5a, cells infected with Ad-DsRed-SP showed a dose-dependent release of cytochrome c into the cytosol as compared with mock and Ad-DsRed-infected cells. Further, Ad-DsRed-SP infection decreased mitochondrial membrane potential in a dose-dependent manner in PNET cells (Supplementary Figure 3). In addition, the role of cathepsin B in mediating cytochrome *c* release was determined by treating Ad-DsRed-SP-infected cells with cathepsin B-specific inhibitor CA-074 Me. Cathepsin B inhibition decreased the SPARC-induced release of cytochorome *c* indicating that the release is due to cathepsin B activity as shown in Figures 5b and c. Collectively, these results place cathepsin B upstream of the mitochondria in the SPARC-induced apoptotic cascade in PNET cells. Cathepsin B was shown to activate Bid.[23] Activated Bid causes the release of cytochrome c from mitochondria and subsequent activation of downstream effector caspases, which carry out the final cleavage steps responsible for the cellular disassembly characteristic of apoptosis.[24] In this study, the role of Bid in SPARC-mediated apoptosis was studied by knocking down *Bid* expression using siRNA. The expression of Bid was markedly suppressed in PNET cells transfected with Bid siRNA but not those with control siRNA (Figure 5d). SPARC-induced release of cytochrome c and cleavage of caspase-3 and PARP were decreased in Bid siRNA-transfected cells compared with SPARC expressed cells transfected with control siRNA (Figure 5d). These findings indicate that cathepsin B induces apoptosis through Bid cleavage in SPARC overexpressed PNET cells.

Exogenous SPARC expression causes tumor growth inhibition in nude mice. To directly evaluate the effect of SPARC on tumor formation *in vivo*, we stereotactically

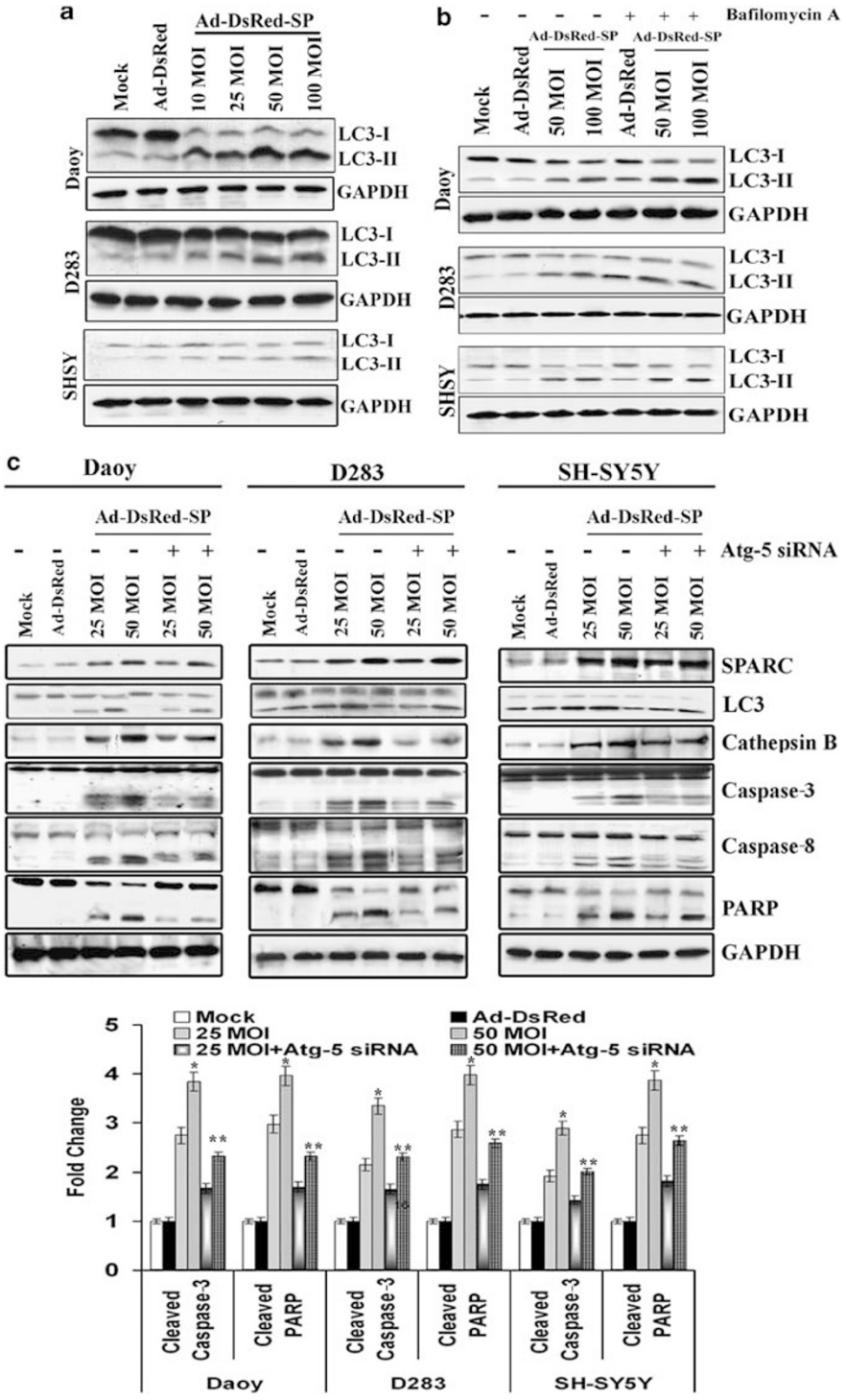

Figure 3 Autophagy vacuoles were observed in SPARC-overexpressed PNET cells. PNET cells were infected with mock, 100 MOI of Ad-DsRed and the indicated MOI of Ad-DsRed-SP for 36 h. (**a**) Cell lysates were used for western blot analysis for LC3-I and LC3-II. (**b**) PNET cells were infected with mock, 100 MOI of Ad-DsRed and the indicated MOI of Ad-DsRed-SP for 24 h and treated with 5 nmol Bafilomycin A1 for further 12 h. Cell lysates were used for western blot analysis for LC3-I and LC3-II. (**c**) PNET cells were infected with mock, 100 MOI of Ad-DsRed, and the indicated MOI of Ad-DsRed-SP and transfected with Atg-5 siRNA. The levels of SPARC, LC3, caspases-3 and -8 and PARP cleavage were assessed by western blot analysis. Results are representative of three independent experiments. GAPDH served as a loading control. The band intensities of cleaved subunits of caspases-3 and cleaved PARP were quantified by densitometry as shown in the corresponding bar graph (means ± S.D.) (columns, mean of three experiments; bars, S.D.). *$P<0.01$, difference between Ad-DsRed and Ad-DsRed-SP 50 MOI treatment; **$P<0.01$; difference between Ad-DsRed-SP 50 MOI and Ad-DsRed-SP 50 MOI + Atg-5 SiRNA

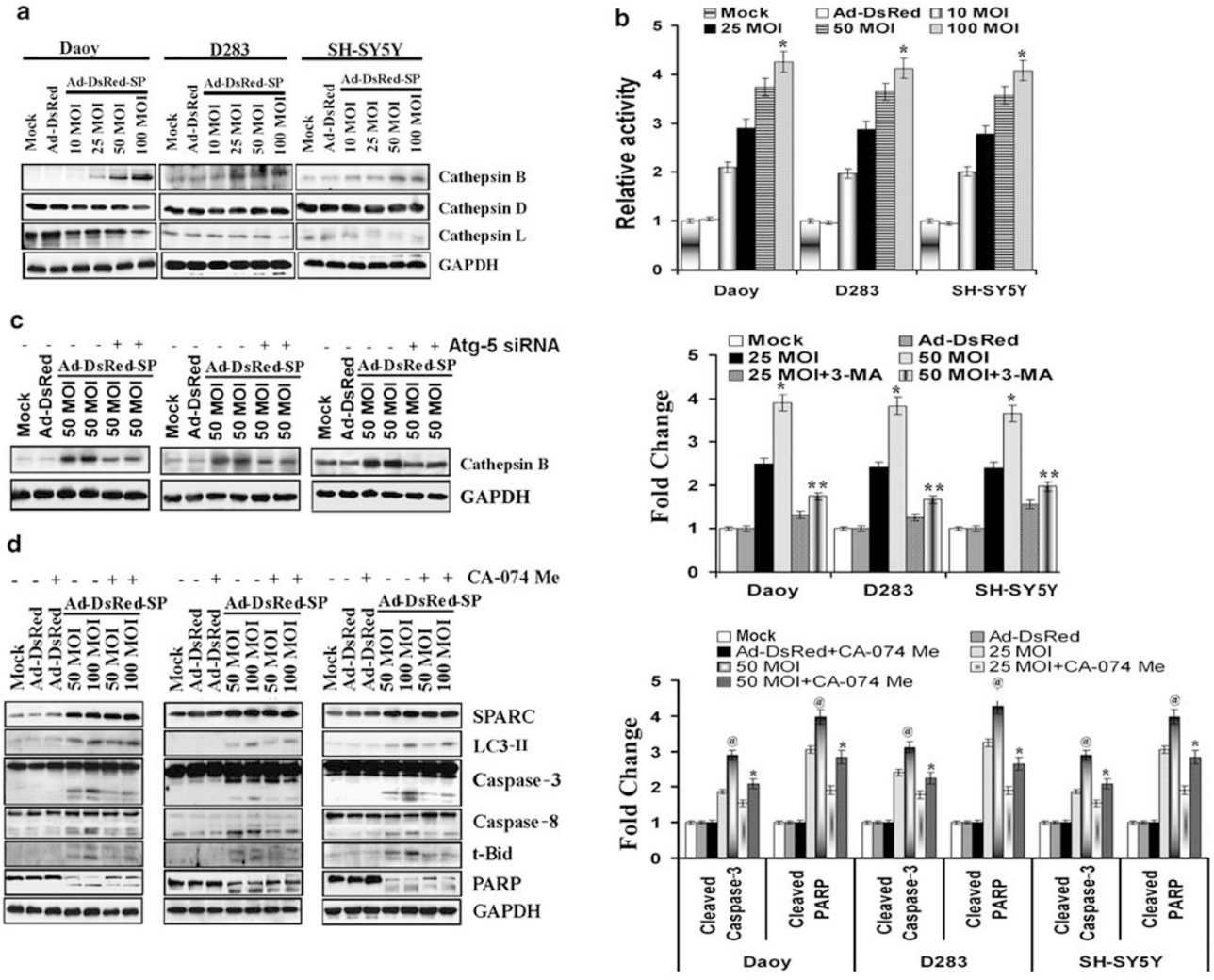

Figure 4 Cathepsin B mediates SPARC-induced apoptosis in PNET cells. PNET cells were infected with mock, 100 MOI of Ad-DsRed and the indicated MOI of Ad-DsRed-SP for 48 h. (**a**) Cathepsin (B, D and L) levels were assessed by western blot analysis in cell lysates. (**b**) PNET cells were infected as mentioned above and Cathepsin B activity was measured. (**c**) PNET cells were infected with mock, 100 MOI of Ad-DsRed and the indicated MOI of Ad-DsRed-SP and treated with autophagy inhibitor, 3-MA. Levels of cathepsin B were determined by western blot analysis. (**d**) PNET cells were infected with mock, 100 MOI of Ad-DsRed and the indicated MOI of Ad-DsRed-SP and treated with 100 μM cathepsin B inhibitor CA-074 Me. Cells were harvested and levels of cleaved caspases-8, -3, PARP and t-Bid were assessed by western blot analysis. Results are representative of three independent experiments. GAPDH served as a loading control (columns, mean of three experiments; bars, S.D.). $^{*}P<0.01$, difference between Ad-DsRed and Ad-DsRed-SP 50 MOI treatment; $^{**}P<0.01$, difference between Ad-DsRed-SP 50 MOI and Ad-DsRed-SP 50 MOI + 3-MA; $^{@}P<0.05$, difference between Ad-DsRed-SP 50 MOI and Ad-DsRed-SP 50 MOI + Ca-074Me

implanted Daoy cells, genetically engineered to express the firefly luciferase gene, intracranially in nude mice. The tumors that arose were challenged with intratumoral injections of Ad-DsRed-SP. Tumor growth was monitored in mice by using *in vivo* imaging system (Xenogen, IVIS, Hopkinton, MA, USA). Representative data are shown in Figure 6a. There was significant decrease in the tumor volume in mice treated with Ad-DsRed-SP compared with mice treated with mock (PBS) and Ad-DsRed. Furthermore, IVIS image analysis also highly correlated with the volume of tumor as assessed by methods described earlier.[25] Histologic analysis of H&E stained tumor sections showed approximately 55–60% reduction of tumor volume ($P\leqslant0.001$) in the brains of mice treated with Ad-DsRed-SP as compared with Ad-DsRed controls (Figure 6b).

To determine whether SPARC caused cathepsin B-mediated apoptosis *in vivo*, tumor sections were immunoassayed for SPARC, cathepsin B and cleaved Bid (t-Bid). Apoptotic content was determined by TUNEL analysis. Figure 6c shows that, consistent with our *in vitro* observations, tumor sections from Ad-DsRed-SP-treated mice showed increased staining for SPARC, cathepsin B and t-Bid. Furthermore, the apoptotic index of tumor cells quantified by the number of positive cells for TUNEL staining, increased with Ad-DsRed-SP treatment (Figure 6d).

Discussion

In this study, we report that SPARC is a strong inducer of autophagy as well as apoptosis. These two processes can be induced in response to cellular stresses in a number of

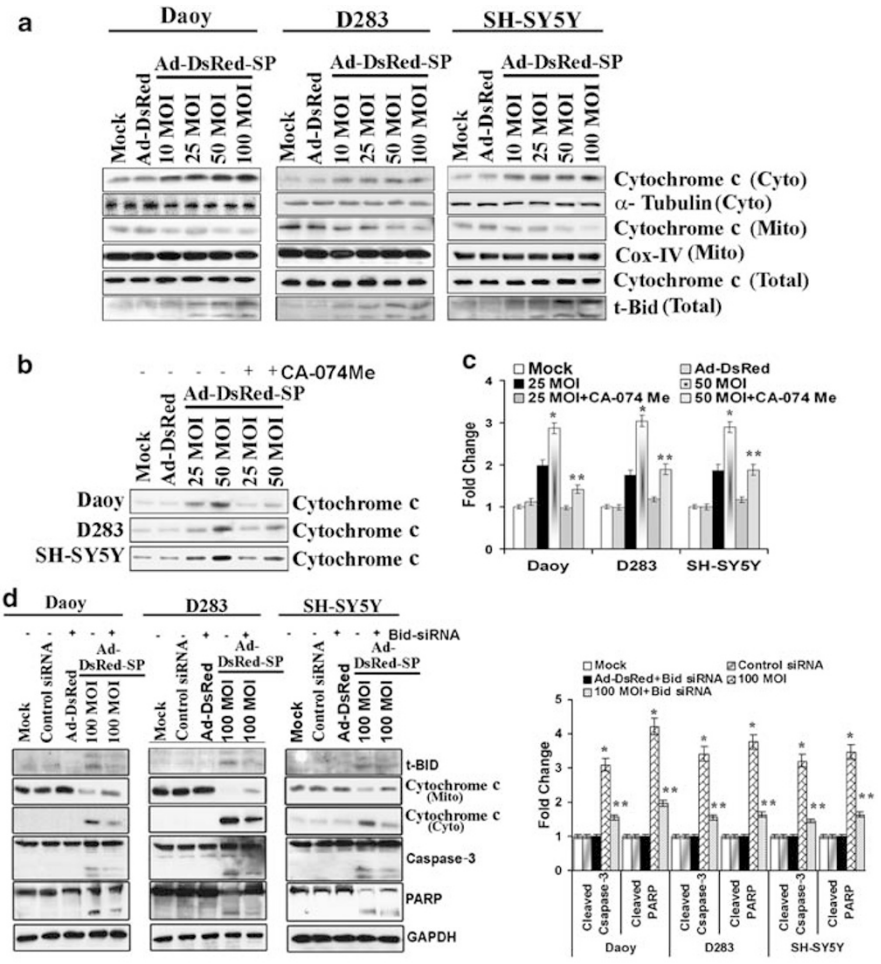

Figure 5 Bid as putative cathepsin B target in SPARC-induced apoptosis. PNET cells were infected with mock, 100 MOI of Ad-DsRed, and the indicated MOI of Ad-DsRed-SP for 48 h. (**a**) Cells were harvested and lysed, and fractions of cytosolic, mitochondrial and total cell lysates were collected separately. These fractions were used for western blot analysis for cytochrome c and t-Bid. α-Tubulin served as a loading control for cytosolic fraction and Cox-IV served as loading control from mitochondrial fractions. (**b**) Cells were harvested after the treatment with cathepsin B inhibitor, and the cytochrome c in the cytosolic fraction was assessed by western blot analysis using anti-cytochrome c antibody. (**c**) Desnitometric analysis for cytochrome c. (**d**) PNET cells were infected with Ad-DsRed-SP at the indicated MOI for 24 h, the cells were then transfected with Bid siRNA and cultured for another 24 h. Cells were harvested and western blot analysis was performed for cytochrome c in the cytosolic fraction. Caspase-3, PARP, LC3 and t-Bid were determined in total cell lysates. GAPDH served as a loading control. Results are representative of three independent experiments (columns, mean of three experiments; bars, S.D.). $^{*}P<0.01$, difference between Ad-DsRed and Ad-DsRed-SP 50 MOI treatment; $^{**}P<0.01$, difference between Ad-DsRed-SP 100 MOI and Ad-DsRed-SP 100 MOI + Bid siRNA

ways such that the induction of autophagy/apoptosis can occur sequentially, simultaneously or in a mutually exclusive manner.[26–28] Our study shows that autophagy develops as a primary response to SPARC expression and then triggers apoptosis in medulloblastoma and neuroblastoma cell lines.

SPARC expression induced several markers of autophagy in human medulloblastoma (Daoy and D283) and neuroblastoma (SH-SY5Y) cells. Cell lysates were analyzed by western blotting to detect both cyto-plasmic LC3-I and its proteolytic derivative LC3-II that preferentially associates with autophagosomal membranes.[29] SPARC triggers an increase of LC3-II with respect to LC3-I in all the three cell lines (Figure 3a). In addition, we used mRFP-LC3 to determine whether SPARC-induced autophagy in PNET cells. Previous studies show that detection of the mRFP-LC3 signal in lysosomes was dependent on autophagy and that autophagy will induce LAMP1 (lysosomal marker), localization with mRFP-LC3 expression.[30] We therefore determined mRFP-LC3 expression in SPARC-overexpressed PNET cells. SPARC overexpression in PNET cells induced autophagy as shown by mRFP-LC3 localization in perinuclear region when compared with mock or Ad-DsRed cells. Further, mRFP-LC3 colocalized with LAMP1 in SPARC overexpressed cells (Supplementary Figure 12). We determined the role of various caspases because we observed an increase in sub-G1 population and an increase in TUNEL-positive cells, in SPARC overexpressed cells. We observed an increase in caspase-8 cleavage and therefore determined the role of this caspase in SPARC-mediated apoptosis. We used caspase-8-specific inhibitor and determined Bid cleavage and cytocrome c release and caspase-3 and PARP cleavage levels. Our data indicate that caspase-8 inhibitor decreased t-Bid and cytochrome c levels suggesting that caspase-8 mediates Bid cleavage in SPARC overexpressed cells (Supplementary

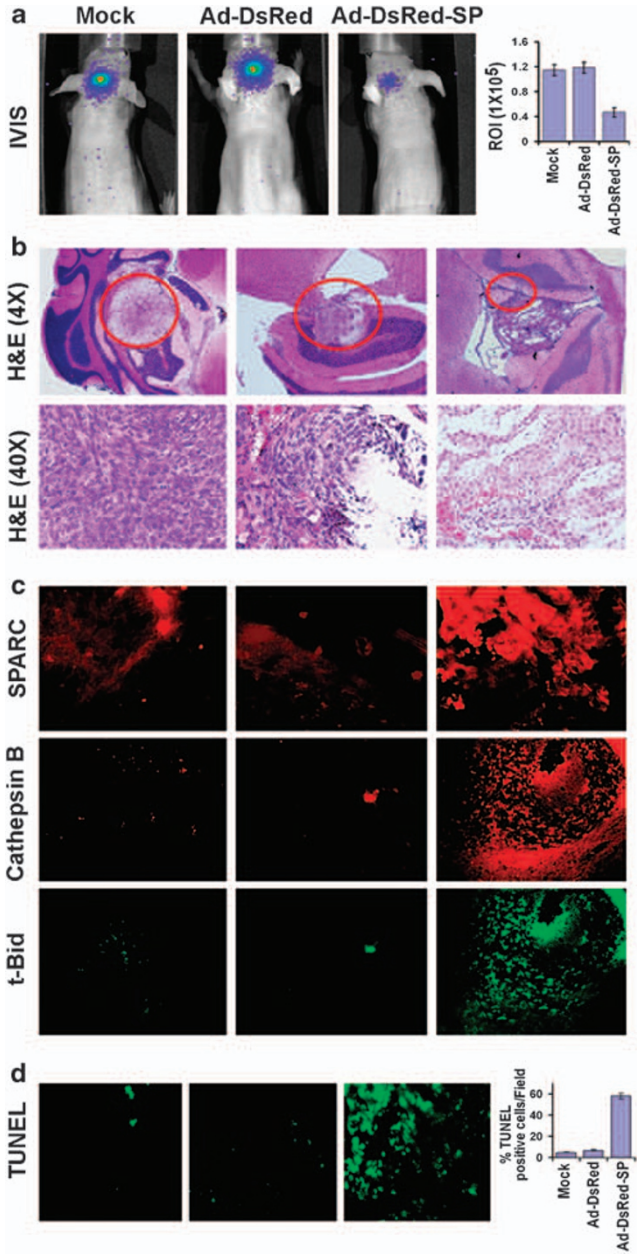

Figure 6 Tumorigenicity *in vivo*. Luciferase-labeled Daoy cells were implanted intracranially in nude mice and treated with intratumoral injections of mock, Ad-DsRed and Ad-DsRed-SP as described in Materials and methods. A total of six animals were studied in each group. (**a**) Noninvasive bioluminescence imaging of luciferase-expressing intracranial Daoy xenografts after six weeks. (**b**) Six weeks later treatment, animals were perfused and the brains harvested and processed. Tissue was stained with H&E per standard protocol (inset 40 ×). Tumor volume is represented graphically by measuring region of interest in IVIS. (**c**) Immunohistochemical analysis of SPARC, cathepsin B and cleaved Bid (t-Bid) expressions in brain sections as described in Materials and methods. Cathepsin B (Red) and t-Bid (Green) are double labeling for the same section. (**d**) Staining for TUNEL was performed on the tumor tissue sections, and representative images of the indicated treatment groups are shown. Arrows indicate representative TUNEL-positive apoptotic cells. The positive-staining apoptotic cells were counted from five sections per tumor tissue from three animals per treatment are represented (ROI, region of interest, columns, mean of three experiments; bars, S.D.)

Figure 13). Further, caspase-8 inhibitor decreased caspase-3 cleavage and activity levels (Supplementary Figure 7) and reversed SPARC-mediated PARP cleavage suggesting that caspase-8 mediates SPARC-induced apoptosis. In addition, caspase-8 inhibitor did not alter SPARC-induced LC3-II levels suggesting that SPARC-induced autophagy is independent of caspase-8 activation (Supplementary Figure 14).

Our results also reveal that SPARC-induced autophagy precedes apoptotic cell death. We show that specific inhibition of autophagy by treatment with 3-methyladenine or Atg siRNA reduced SPARC-mediated apoptosis. There is evidence that over-stimulation of autophagy can lead to cell death, possibly through activating apoptosis.[31] Previous findings that suggest autophagy as a reflection of the therapeutic efficacy of anti-neoplastic agents are: the persistent activation of autophagy can lead to programmed cell death[32] and that the autophagy regulator beclin 1 (*BECN1*) is a haploinsufficient tumor-suppressor gene that induces autophagy when overexpressed.[33] It is likely that excessive autophagy destroys a large amount of protein and organelles which, beyond a certain threshold, causes a bioenergetic catastrophe culminating in cell death.[34] H_2O_2 and 2-methoxyestradiol (2-ME) induce apoptosis in cells and have recently been shown to induce autophagy leading to cell death in HEK293 and U87 cells.[35] This group also found that inhibition of autophagy significantly reduces H_2O_2 or 2-ME-mediated cell death.

Our study provides the first *in vitro* evidence that cathepsin B is a molecular link between autophagy and apoptosis in SPARC-expressing cells. SPARC expression-induced cathepsin B expression in PNET cells. Cathepsin B, a lysosomal cysteine protease, has recently been implicated in apoptosis.[36] Lysosomal permeabilization with release of cathepsin B into the cytosol has been associated with mitochondrial dysfunction and caspase-dependent cell death in hepatocytes.[37] SPARC-induced cathepsin B expression is associated with cytochrome c release and caspase-dependent death in PNET cells. Blocking cathepsin B with a cathepsin B-specific inhibitor prevented SPARC-induced apoptosis, but it did not affect autophagy, thereby suggesting that autophagy induces cathepsin B-mediated apoptosis in SPARC-expressing PNET cells. Previous work showed that SPARC potentiated apoptosis by increasing caspase-8 signaling.[38] Our work shows that SPARC-induced autophagy-mediated cathepsin B induction, which in turn induced caspase-8-mediated apoptosis; because inhibition of autophagy reversed SPARC-induced caspase-8-mediated apoptosis. We also show that the brain sections of mice that received Ad-DsRed-SP treatment show remarkable increases in the levels of cathepsin B expression and TUNEL-positive cells as compared with the brain sections of control and Ad-DsRed-treated mice. These results suggest cathepsin B mediates apoptosis *in vivo*. Studies from other laboratories have also implicated cathepsin B in apoptosis. Pharmacologic inhibition of cathepsin B has been reported to block apoptosis induced by p53 and cytotoxic agents.[39] Redistribution of cathepsin B from vesicles to the cytosol has also been shown in neurons undergoing death after global ischemia.[40] Cathepsin B was shown to contribute to TNF-α-mediated apoptosis by promoting mitochondrial release of cytochrome c in hepatocytes.[36]

Further experiments were performed to determine how cathepsin B might be affecting this apoptotic cascade in Ad-DSRed-SP-infected cells. The cathepsin proteases could induce apoptosis by a variety of different mechanisms.[41] One possibility is that cathepsins could nonspecifically degrade important cellular proteins, thereby causing the cell to initiate apoptosis.[42] Alternately, cathepsins can directly cleave caspase zymogens and caspases (e.g., caspase-3).[43] Another mode of cathepsin action places cathepsins far upstream in the apoptotic cascade, cleaving the pro-apoptotic Bcl-2 family member Bid to initiate mitochondrial release of cytochrome c. We found clear evidence for Bid cleavage/activation in SPARC overexpressed cells. We therefore tested whether the pro-apoptotic signaling by lysosomal cathepsin B proceeds through the pro-apoptotic Bcl-2 family member Bid in SPARC overexpressed cells. Transfection with Bid siRNA before Ad-DsRed-SP infection inhibited SPARC-induced apoptosis suggesting that Bid is the putative target for cathepsin B-mediated apoptosis in SPARC-induced cells. Similarly, cathepsin B and its substrate Bid were shown to be molecular links between apoptosis and autophagy in breast cancer MCF-7 cells exposed to the cytostatic drug, camptothecin (inhibitor of DNA topoisomerase I).[35]

In conclusion, we show for the first time that autophagy and apoptosis are sequentially triggered by SPARC through the cathepsin B-mediated, mitochondria-dependent pathway (Scheme 1). This conclusion is based on three lines of argumentation: (1) inhibition of autophagy using 3-MA/Atg-5 siRNA decreased SPARC-mediated apoptosis; (2) inhibition of autophagy using 3-MA/Atg-5 siRNA blocked SPARC-induced cathepsin B; and (3) inhibition of cathepsin B did not alter autophagy but inhibited cytochrome c-mediated apoptosis in SPARC overexpressed cells.

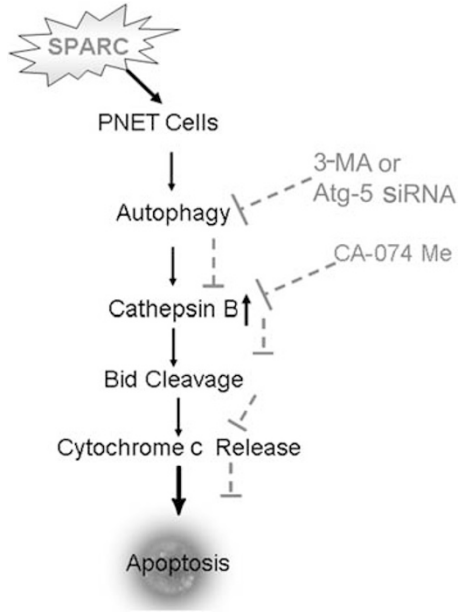

Scheme 1 Flow diagram. Schematic representation of the sequence of events leading to apoptosis because of overexpression of SPARC in PNET cells. In this figure, we show for the first time that autophagy and apoptosis are sequentially triggered by SPARC through the cathepsin B-mediated, mitochondria-dependent apoptotic pathway

Materials and Methods

Cell cultures. We used the Daoy (ATCC #HTB 186), D283 Med (ATCC #HTB 185), and SH-SY5Y (ATCC #CRL 2266) cell lines. Daoy cells were cultured in Advanced-MEM, D283 cells were cultured in Advanced-MEM (Zn option medium without phenol red), and SH-SY5Y cells were cultured in advanced DMEM. All of the above media were supplemented with 5% fetal bovine serum, 2 mM L-glutamine, 2 mM sodium pyruvate, 100 units/ml penicillin and 100 μg/ml streptomycin. Cells were maintained in a humidified atmosphere containing 5% CO_2 at 37 °C.

Antibodies and reagents. Antibodies against SPARC, caspase-3, t-Bid, cytochrome c, MAP- LC3, cathepsin D, cathepsin L and GAPDH were obtained from Santa Cruz Biotechnology (Santa Cruz, CA, USA). Antibodies against caspase-8, LC-3 (Cell Signaling Technology, Beverly, MA, USA), PARP (EMD Biosciences, San Diego, CA, USA) and cathepsin B (Athens Research and Technology, Athens, GA, USA) were also used in this study. Bid siRNA and Atg-5 siRNA were obtained from Santa Cruz Biotechnology. pmRFP-LC3 (Addgene plasmid 21075) was obtained from Addgene Inc. (Cambridge, MA, USA). The autophagy inhibitor (3-MA), cathepsin B inhibitor (CA-074 Me) and the caspase 8 inhibitor (IETD-Fmk) were obtained from Calbiochem (San Diego, CA, USA).

Adenovirus construction. We constructed two adenoviral vectors, one carrying full-length human SPARC cDNA (Ad-Dsred-SP) and an empty vector (Ad-DsRed) using Adeno-X ViraTrak Expression System 2 (Clontech Laboratories, Mountain View, CA, USA). SPARC cDNA was cloned in to pDNR-CMV donor vector as per manufacturer's protocol. To ensure that the correct restriction fragment was cloned, the following compatible restriction sites were added: Xho I at the 5′ end and Xba I at the 3′ end of the primer sequences. The donor vector is the used for recombination with pLP-Adeno-X-CMV-E3-DsRed-Express Vector (acceptor vector) using Cre Recombinase as per manufacturer's protocol. The donor vector's two loxP sites flank the 5′ end of the MCS and the 5′ end of the chloramphenicol resistance gene (Cmr), and mediate the transfer of these intervening sequences into the acceptor vector. After the Cre-loxP reaction, the recombinant pLP-Adeno-X plasmid can then be used to generate recombinant adenovirus for strong, constitutive expression of the gene. The recombined vector was then digested with *Pac*I enzyme to expose the inverted terminal repeats located at either end of the genome plasmid and to produce virus particles. The adenovirus-containing SPARC cDNA was termed Ad-DsRed-SP and the virus without SPARC cDNA was termed Ad-DsRed. Adenovirus generation, amplification and titer were performed according to previously described procedures.[44] Briefly, viral particles were purified using a cesium chloride density gradient. Viral titers were assessed using the plaque-forming unit (PFU) and by counting infectious virus particles.

Adenoviral infection. Infection with recombinant viruses was accomplished by exposing cells to adenovirus in serum-free cell culture medium for 1 h followed by addition of serum-containing medium. Cells were then incubated for varying time periods (as detailed in the following experiments). We used Ad-DsRed recombinant adenovirus as a vector control.

Western blotting. Western blot analysis was performed as described earlier.[45] Briefly, PNET cells were cultured in 100 mm plates and infected with mock, 100 MOI of Ad-DsRed, or various MOI of Ad-DsRed-SP and incubated for 48 h at 37 °C. Cell lysates were prepared in radioimmunoprecipitation assay buffer and protein concentrations were measured using bicinchoninic acid protein assay regents (Pierce, Rockford, IL, USA). Equal amounts of protein was resolved on SDS-PAGE gel and transferred on to PVDF membrane. Next, the blot was blocked and probed overnight with different primary antibodies at 4 °C followed by HRP-conjugated secondary antibodies for 1 h and signals were detected by using ECL reagent.

RT-PCR. PNET cells were cultured in 100 mm plates and infected with mock, 100 MOI of Ad-DsRed, or various MOI of Ad-DsRed-SP and incubated for 36 h at 37 °C. Total RNA was extracted from cells as described by Chomczynski and Sacchi.[46] The solution was then treated with DNase I (Ambion, Austin, TX, USA) for 30 min at 37 °C. PCR was performed using an RT-PCR kit (Invitrogen, Carlsbad, CA, USA) as follows: 35 cycles of denaturation at 94 °C for 1 min, annealing at 67 °C for 30 s and extension at 72 °C for 90 s. The expected PCR products were resolved on 2% agarose gels and visualized using ethidium bromide staining. To normalize for the amount of input RNA, RT-PCR was performed with primers for the constitutively expressed GAPDH. SPARC primers, sense 5′-GGAAGAAACTGTGGCAGAGG-3′ and antisense 5′-ATTGCTGCACACCTTCTCAA-3, and GAPDH primers sense

5-TGAAGGTCGGAGTCAACGGATTTGGT-3 and antisense 5-CATGTGGGCCAT GAGGTCCACCAC-3.

Flow cytometry. For assessment of DNA content, PNET cells were plated overnight in 100 mm tissue culture plates and infected for 48 h as described above. We used FACS analysis that uses propidium iodide staining of nuclear DNA to characterize hypo-diploid cells.[47] Briefly, cells were harvested by trypsinization and stained with propidium iodide (2 mg/ml) in 4 mM sodium citrate containing 3% (w/v) Triton X-100 and RNase A (0.1 mg/ml; Sigma, St. Louis, MO, USA). Suspensions of 2×10^6 cells were analyzed by FACS Caliber System (Becton Dickinson Bioscience, San Jose, CA, USA) with laser excitation at 488 nm using an emission 639 nm band pass filter to collect the red propidium iodide fluorescence. The percentages of cells in the various phases of the cell cycle, namely, sub-G_0/G_1, G_0/G_1, S, and G_2/M, were assessed using Cell Quest software (Becton Dickinson Bioscience).

TUNEL assay. To evaluate the apoptotic response of Ad-DsRed-SP, we performed terminal deoxynucleotide transferase (TdT)-mediated biotin-dUTP nick end labeling (TUNEL) using the commercially available *in situ* cell death detection kit (Roche, Indianapolis, IN, USA). Briefly, 5000 cells were seeded onto eight-well chamber slides and infected with mock, 100 MOI of Ad-DsRed, or various MOIs of Ad-DsRed-SP. After 48 h of infection, the cells were washed and fixed with 4% buffered para-formaldehyde and permeabilized with freshly prepared 0.1% Triton-X100, 0.1% sodium citrate solution. These cells were then incubated with TUNEL reaction mixture for 1 h at 37 °C in a humidified chamber. The slides were washed three times with PBS and the incorporated biotin-dUTP was detected under a fluorescence microscope. For the paraffin-embedded tissue sections, slides were dewaxed, rehydrated and permeabilized according to the standard protocols and processed as above.

Transfection with plasmids. All transfection experiments were performed using fuGene *HD* transfection reagent according to the manufacturer's protocol (Roche). Briefly, plasmid/siRNA was mixed with fuGene *HD* reagent (1 : 3 ratio) in 500 μl of serum-free medium and left for 30 min to allow for complex formation. The complex was then added to the 100 mm plate, which had 2.5 ml of serum-free medium (2 μg plasmid per ml of medium). After 6 h of transfection, complete medium was added, and cultured for another 24 h.

Measurement of cathepsin B activity. Cathepsin B activity was measured by cathepsin B activity assay kit (BioVision, Mountain View, CA, USA). Briefly, cells were washed with the PBS, and lysed in chilled cathepsin B cell lysis buffer. After incubation on ice for 10 min, 10 mM cathepsin B substrate (Ac-RR-AFC, 200 μM final concentration) was added and incubated at 37 °C for 2 h as indicated in manufacturer's protocol. The release of free amino-4-trifluoromethyl coumarin was monitored in a fluorometer (Fluoroskan ascent, Thermo LabSystems, Waltham, MA, USA) with a 409 nm excitation filter and 515 nm emission filter.[48]

Measurement of caspase-3 and caspase-8 activity. The caspase-3 and -8 activity assays were performed using specific colorimetric activity assay kits (Chemicon International, Billerica, MA, USA) as per the manufacturer's instructions. Briefly, samples were resuspended in chilled cell lysis buffer and incubated on ice for 10 min. After centrifugation, the cytosolic extract was collected, and the assay mixture was prepared in a 96-well plate. To further confirm the specificity of casapse-3 or -8 activity, the samples were preincubated with the caspase-3 or -8 inhibitors sample for 30 min at room temperature before adding the caspase-3 substrate solution. Assay mixtures were incubated for 2 h at 37 °C, and caspase activities were measured by reading the absorbance of their products at 405 nm in a microtiter plate reader.

Transmission electron microscopy. Cells were fixed in 2.5% glutaraldehyde in 0.1 M cacodylic buffer, pH 7.4 for 2 h at 4 °C, washed in 0.1 M cacodylic buffer (pH 7.4) overnight, and post-fixed with 1% osmium tetroxide with 0.8% K_4FeCN_6 in cacodylic buffer for 1 h at room temperature. The samples were dehydrated in an ethanol gradient (30, 50, 70, 80, 90, 96 and 100%) and propylene oxide and then embedded in Epon 812. The blocks were cut with Reichert OM3 ultramicrotome and stained with 9% uranyl acetate and lead citrate (0.2%) solution. Sections were photographed using a JEOL JEM 1 OOC transmission electron microscope (JEOL USA, Inc, Peabody, MA, USA).

Detection of AVOs by acridine orange. Autophagy vacuolization was visualized by acridene orange as described by Paglin *et al*.[15] Briefly, PNET cells were seeded in 100 mm and were infected with Ad-DsRed-SP as described above. At the appropriate time points, cells were incubated with 1 mg/ml acridine orange (Molecular Probes, Eugene, OR, USA) in serum-free medium for 15 min. The acridine orange was removed and fluorescent micrographs were obtained using an inverted fluorescence microscope. The cytoplasm and nucleus of the stained cells fluoresced bright green, whereas the acidic AVOs fluoresced bright red.

Cell fractionation and isolation of mitochondria. All procedures were performed at 4 °C. Controls and Ad-DsRed-SP-treated PNET cells were harvested, washed in PBS and then suspended in isotonic sucrose buffer (PES) composed of 10 mM phosphate buffer, pH 7.2, 1 mM EDTA, 1 mM EGTA, 1 mM $MgCl_2$, 250 mM sucrose, 1 mg/ml pepstatin, 1 mg/ml leupeptin and 40 mg/ml PMSF. Cell homogenates examined by cytospin and Diff-Quick staining showed that; 90% of the cells had been disrupted. The homogenates were centrifuged twice at 800 *g* for 10 min to remove nuclei and any residual intact cells. The postnuclear supernatant was centrifuged at 10 000 *g* for 20 min. The pellet (crude mitochondrial fraction) was washed with PBS two times to remove the sucrose. The 10 000 *g* supernatant was centrifuged at 100 000 *g* for 30 min and the resulting supernatant was used as the cytosolic fraction. Subcellular fractionation was confirmed by assaying citrate synthase activity as a marker for the mitochondrial matrix. Lactate dehydrogenase was used as a marker for the cytosolic fraction and was assayed using a kit from Roche Biochemicals (Roche). For protein measurements, mitochondria were subjected to three freeze–thaw cycles using liquid N_2 and a 37 °C water bath. Protein was measured with the Bio-Rad protein assay kit (Bio-Rad Laboratories, Hercules, CA, USA) using bovine serum albumin as the standard.

Transmembrane potential of the mitochondria. The MitoLight apoptosis detection kit (Chemicon International Inc., Temecula, CA, USA) was used as per manufacturer's instructions. Briefly, PNET cells treated were grown in eight-well chamber slides and infected with AdDsred-SP as described above. After 48 h, the chamber slides were covered with diluted MitoLight reagent solution and incubated for 20 min in a 5% CO_2 incubator at 37 °C. The solution was then replaced with the pre-warmed incubation buffer, and the cells were immediately observed under a fluorescence microscope using an IB cube filter (excitation at 460–490 nm; emission at 515 nm) (IX70-FLA). The fluorescent reagent can be accumulated into the mitochondria of healthy cells and aggregates to generate red fluorescence (excitation at 585 nm; emission at 590 nm). However, in the apoptotic cells, the reagent remains monomer in the cytoplasm, and is fluorescent green (excitation at 510 nm; emission at 527 nm).

Intracranial tumor model. The Institutional Animal Care and Use Committee at the University of Illinois College of Medicine-Peoria approved all experimental procedures involving the use of animals. A small, hand-controlled twist drill was used to make the hole, and a specially devised screwdriver was used to thread and secure the screw into the hole. After a recovery period of 5 days, nude mice were anesthetized and Daoy cells (1×10^5 cells/5 μl PBS), stably transfected for luc expression, were stereotactically implanted as described elsewhere with minor modifications.[49] Two weeks after tumor cell implantation, the animals were randomized into three groups (six animals per group). Each mouse received three intratumoral injections on days 15, 16 and 17. Group 1 received PBS (6 μl; $n = 6$). Group 2 received 5×10^7 PFU of Ad-DsRed virus in 6 μl of PBS. Group 3 received 5×10^7 PFU of Ad-DsRed-SP in 5 μl of PBS. Animals, which lost $\geqslant$20% of body weight or had trouble ambulating, feeding or grooming, were killed. Animals were monitored for up to 90 days, which is when we arbitrarily terminated the experiment. Tumor growth was monitored using *in vivo* imaging system (IVIS) every alternate day till the study termination. Mice brains were fixed in 10% buffered formalin and embedded in paraffin. Tissue sections (5 μm thick) were obtained from the paraffin blocks and stained with H&E using standard histological techniques. Tissue sections were also subjected to immunostaining with antibodies for SPARC, cathepsin B and t-Bid. After adding FITC or Texas Red conjugated secondary antibody, sections were counterstained with DAPI, and negative control slides were obtained by nonspecific IgG as the primary antibody. After mounting in an anti-fade mounting solution (Invitrogen), the samples were analyzed with a fluorescence microscope.

Statistical analyses. All data are expressed as mean ± S.D. Statistical analysis was performed using the Student's *t*-test or a one-way analysis of variance. $P < 0.05$ was considered significant.

Conflict of interest

Dr Lakka's work was funded by NIH. The remaining authors declare no conflict of interest.

Acknowledgements. We thank Shellee Abraham for paper preparation, Diana Meister and Sushma Jasti for paper review and Professor T Yoshimori for providing pmRFP-LC3 plasmid. This research was supported by National Cancer Institute Grant CA132853 (to SL). Contents of this paper are solely the responsibility of the authors and do not necessarily represent the official views of NIH.

1. Klionsky DJ, Emr SD. Autophagy as a regulated pathway of cellular degradation. *Science* 2000; **290**: 1717–1721.
2. Xue L, Fletcher GC, Tolkovsky AM. Autophagy is activated by apoptotic signalling in sympathetic neurons: an alternative mechanism of death execution. *Mol Cell Neurosci* 1999; **14**: 180–198.
3. Espert L, Denizot M, Grimaldo M, Robert-Hebmann V, Gay B, Varbanov M *et al.* Autophagy is involved in T cell death after binding of HIV-1 envelope proteins to CXCR4. *J Clin Invest* 2006; **116**: 2162–2172.
4. Katayama M, Kawaguchi T, Berger MS, Pieper RO. DNA damaging agent-induced autophagy produces a cytoprotective adenosine triphosphate surge in malignant glioma cells. *Cell Death Differ* 2007; **14**: 548–558.
5. Levine B, Kroemer G. Autophagy in the pathogenesis of disease. *Cell* 2008; **132**: 27–42.
6. Degenhardt K, Mathew R, Beaudoin B, Bray K, Anderson D, Chen G *et al.* Autophagy promotes tumor cell survival and restricts necrosis, inflammation, and tumorigenesis. *Cancer Cell* 2006; **10**: 51–64.
7. Lum JJ, Bauer DE, Kong M, Harris MH, Li C, Lindsten T *et al.* Growth factor regulation of autophagy and cell survival in the absence of apoptosis. *Cell* 2005; **120**: 237–248.
8. Jin S, DiPaola RS, Mathew R, White E. Metabolic catastrophe as a means to cancer cell death. *J Cell Sci* 2007; **120**: 379–383.
9. DiPaola RS, Dvorzhinski D, Thalasila A, Garikapaty V, Doram D, May M *et al.* Therapeutic starvation and autophagy in prostate cancer: a new paradigm for targeting metabolism in cancer therapy. *Prostate* 2008; **68**: 1743–1752.
10. White E, DiPaola RS. The double-edged sword of autophagy modulation in cancer. *Clin Cancer Res* 2009; **15**: 5308–5316.
11. Yiu GK, Chan WY, Ng SW, Chan PS, Cheung KK, Berkowitz RS *et al.* SPARC (secreted protein acidic and rich in cysteine) induces apoptosis in ovarian cancer cells. *Am J Pathol* 2001; **159**: 609–622.
12. Puolakkainen PA, Brekken RA, Muneer S, Sage EH. Enhanced growth of pancreatic tumors in SPARC-null mice is associated with decreased deposition of extracellular matrix and reduced tumor cell apoptosis. *Mol Cancer Res* 2004; **2**: 215–224.
13. DiMartino JF, Lacayo NJ, Varadi M, Li L, Saraiya C, Ravindranath Y *et al.* Low or absent SPARC expression in acute myeloid leukemia with MLL rearrangements is associated with sensitivity to growth inhibition by exogenous SPARC protein. *Leukemia* 2006; **20**: 426–432.
14. Susin SA, Lorenzo HK, Zamzami N, Marzo I, Snow BE, Brothers GM *et al.* Molecular characterization of mitochondrial apoptosis-inducing factor. *Nature* 1999; **397**: 441–446.
15. Paglin S, Hollister T, Delohery T, Hackett N, McMahill M, Sphicas E *et al.* A novel response of cancer cells to radiation involves autophagy and formation of acidic vesicles. *Cancer Res* 2001; **61**: 439–444.
16. Mizushima N. Methods for monitoring autophagy. *Int J Biochem Cell Biol* 2004; **36**: 2491–2502.
17. Kabeya Y, Mizushima N, Ueno T, Yamamoto A, Kirisako T, Noda T *et al.* LC3, a mammalian homologue of yeast Apg8p, is localized in autophagosome membranes after processing. *EMBO J* 2000; **19**: 5720–5728.
18. Yousefi S, Perozzo R, Schmid I, Ziemiecki A, Schaffner T, Scapozza L *et al.* Calpain-mediated cleavage of Atg5 switches autophagy to apoptosis. *Nat Cell Biol* 2006; **8**: 1124–1132.
19. Seglen PO, Gordon PB. 3-Methyladenine: specific inhibitor of autophagic/lysosomal protein degradation in isolated rat hepatocytes. *Proc Natl Acad Sci USA* 1982; **79**: 1889–1892.
20. Leist M, Jaattela M. Four deaths and a funeral: from caspases to alternative mechanisms. *Nat Rev Mol Cell Biol* 2001; **2**: 589–598.
21. Salvesen GS. A lysosomal protease enters the death scene. *J Clin Invest* 2001; **107**: 21–22.
22. Guicciardi ME, Miyoshi H, Bronk SF, Gores GJ. Cathepsin B knockout mice are resistant to tumor necrosis factor-alpha-mediated hepatocyte apoptosis and liver injury: implications for therapeutic applications. *Am J Pathol* 2001; **159**: 2045–2054.
23. Cirman T, Oresic K, Mazovec GD, Turk V, Reed JC, Myers RM *et al.* Selective disruption of lysosomes in HeLa cells triggers apoptosis mediated by cleavage of Bid by multiple papain-like lysosomal cathepsins. *J Biol Chem* 2004; **279**: 3578–3587.
24. Luo X, Budihardjo I, Zou H, Slaughter C, Wang X. Bid, a Bcl2 interacting protein, mediates cytochrome c release from mitochondria in response to activation of cell surface death receptors. *Cell* 1998; **94**: 481–490.
25. Ding Q, Grammer JR, Nelson MA, Guan JL, Stewart Jr JE, Gladson CL. p27Kip1 and cyclin D1 are necessary for focal adhesion kinase regulation of cell cycle progression in glioblastoma cells propagated *in vitro* and *in vivo* in the scid mouse brain. *J Biol Chem* 2005; **280**: 6802–6815.
26. Gorski SM, Chittaranjan S, Pleasance ED, Freeman JD, Anderson CL, Varhol RJ *et al.* A SAGE approach to discovery of genes involved in autophagic cell death. *Curr Biol* 2003; **13**: 358–363.
27. Herman-Antosiewicz A, Johnson DE, Singh SV. Sulforaphane causes autophagy to inhibit release of cytochrome C and apoptosis in human prostate cancer cells. *Cancer Res* 2006; **66**: 5828–5835.
28. Kanzawa T, Ito H, Kondo Y, Kondo S. Current and future gene therapy for malignant gliomas. *J Biomed Biotechnol* 2003; **2003**: 25–34.
29. Kabeya Y, Mizushima N, Yamamoto A, Oshitani-Okamoto S, Ohsumi Y, Yoshimori T. LC3, GABARAP and GATE16 localize to autophagosomal membrane depending on form-II formation. *J Cell Sci* 2004; **117**: 2805–2812.
30. Kimura S, Noda T, Yoshimori T. Dissection of the autophagosome maturation process by a novel reporter protein, tandem fluorescent-tagged LC3. *Autophagy* 2007; **3**: 452–460.
31. Scott RC, Juhasz G, Neufeld TP. Direct induction of autophagy by Atg1 inhibits cell growth and induces apoptotic cell death. *Curr Biol* 2007; **17**: 1–11.
32. Yu L, Lenardo MJ, Baehrecke EH. Autophagy and caspases: a new cell death program. *Cell Cycle* 2004; **3**: 1124–1126.
33. Qu X, Yu J, Bhagat G, Furuya N, Hibshoosh H, Troxel A *et al.* Promotion of tumorigenesis by heterozygous disruption of the beclin 1 autophagy gene. *J Clin Invest* 2003; **112**: 1809–1820.
34. Mizushima N, Levine B, Cuervo AM, Klionsky DJ. Autophagy fights disease through cellular self-digestion. *Nature* 2008; **451**: 1069–1075.
35. Chen Y, Millan-Ward E, Kong J, Israels SJ, Gibson SB. Oxidative stress induces autophagic cell death independent of apoptosis in transformed and cancer cells. *Cell Death Differ* 2008; **15**: 171–182.
36. Guicciardi ME, Deussing J, Miyoshi H, Bronk SF, Svingen PA, Peters C *et al.* Cathepsin B contributes to TNF-alpha-mediated hepatocyte apoptosis by promoting mitochondrial release of cytochrome c. *J Clin Invest* 2000; **106**: 1127–1137.
37. Werneburg NW, Guicciardi ME, Bronk SF, Gores GJ. Tumor necrosis factor-alpha-associated lysosomal permeabilization is cathepsin B dependent. *Am J Physiol Gastrointest Liver Physiol* 2002; **283**: G947–G956.
38. Tang MJ, Tai IT. A novel interaction between procaspase 8 and SPARC enhances apoptosis and potentiates chemotherapy sensitivity in colorectal cancers. *J Biol Chem* 2007; **282**: 34457–34467.
39. Lotem J, Peled-Kamar M, Groner Y, Sachs L. Cellular oxidative stress and the control of apoptosis by wild-type p53, cytotoxic compounds, and cytokines. *Proc Natl Acad Sci USA* 1996; **93**: 9166–9171.
40. Hill IE, Preston E, Monette R, MacManus JP. A comparison of cathepsin B processing and distribution during neuronal death in rats following global ischemia or decapitation necrosis. *Brain Res* 1997; **751**: 206–216.
41. Turk B, Stoka V, Rozman-Pungercar J, Cirman T, Droga-Mazovec G, Oresic K *et al.* Apoptotic pathways: involvement of lysosomal proteases. *Biol Chem* 2002; **383**: 1035–1044.
42. Williams MS, Henkart PA. Apoptotic cell death induced by intracellular proteolysis. *J Immunol* 1994; **153**: 4247–4255.
43. Vancompernolle K, Van Herreweghe F, Pynaert G, Van de Craen M, DeVos K, Totty N *et al.* Atractyloside-induced release of cathepsin B, a protease with caspase-processing activity. *FEBS Lett* 1998; **438**: 150–158.
44. Mohan PM, Barve M, Chatterjee A, Hosur RV. pH driven conformational dynamics and dimer-to-monomer transition in DLC8. *Protein Sci* 2006; **15**: 335–342.
45. Bhoopathi P, Chetty C, Kunigal S, Vanamala SK, Rao JS, Lakka SS. Blockade of tumor growth due to matrix metalloproteinase-9 inhibition is mediated by sequential activation of beta1-integrin, ERK, and NF-kappaB. *J Biol Chem* 2008; **283**: 1545–1552.
46. Chomczynski P, Sacchi N. Single-step method of RNA isolation by acid guanidinium thiocyanate-phenol-chloroform extraction. *Anal Biochem* 1987; **162**: 156–159.
47. Healy E, Dempsey M, Lally C, Ryan MP. Apoptosis and necrosis: mechanisms of cell death induced by cyclosporine A in a renal proximal tubular cell line. *Kidney Int* 1998; **54**: 1955–1966.
48. Ha SD, Martins A, Khazaie K, Han J, Chan BM, Kim SO. Cathepsin B is involved in the trafficking of TNF-alpha-containing vesicles to the plasma membrane in macrophages. *J Immunol* 2008; **181**: 690–697.
49. Lal S, Lacroix M, Tofilon P, Fuller GN, Sawaya R, Lang FF. An implantable guide-screw system for brain tumor studies in small animals. *J Neurosurg* 2000; **92**: 326–333.

Supplementary Information accompanies the paper on Cell Death and Differentiation website (http://www.nature.com/cdd)